Chapter 3

A dry electrode-based compact-sized sEMG Sensor for myoelectric hand prosthesis

3.1 Introduction

Measurement of surface electromyography (sEMG) signals requires the use of myoelectrodes and appropriate preprocessing circuitry (Drost et al. 2006). The quality of the sEMG signal for controlling prosthesis mainly relies on factors like electrode type, its placement on the skin, and the preprocessing circuitry (Shobaki et al. 2013; Imtiaz et al. 2013). Surface myoelectrodes give the basic assessment of the EMG signal under the skin. These are categorized into wet and dry type electrodes (Figure 3.1). Silver-silver chloride (Ag/AgCl) is a wet type electrode that provides good signal quality and low electrode-skin impedance but has some limitations. These electrodes may cause irritations and allergies to the skin, and their long-time use can degrade the quality of the signal because the gel in the electrode dries with time. Moreover, these require skin preparation, which increases the time and cost of measurement (Baek et al. 2008; Pylatiuk et al. 2009). These limitations make the wet electrodes unsuitable for prosthetic application. On the other hand, dry electrodes do not require gel or skin preparation procedures, reducing time and effort to set up. Although these electrodes may have higher skin-electrode impedance and may be susceptible to motion artifacts, there is a possibility of getting stronger sEMG signals with these electrodes (Searle and Kirkup 2000).

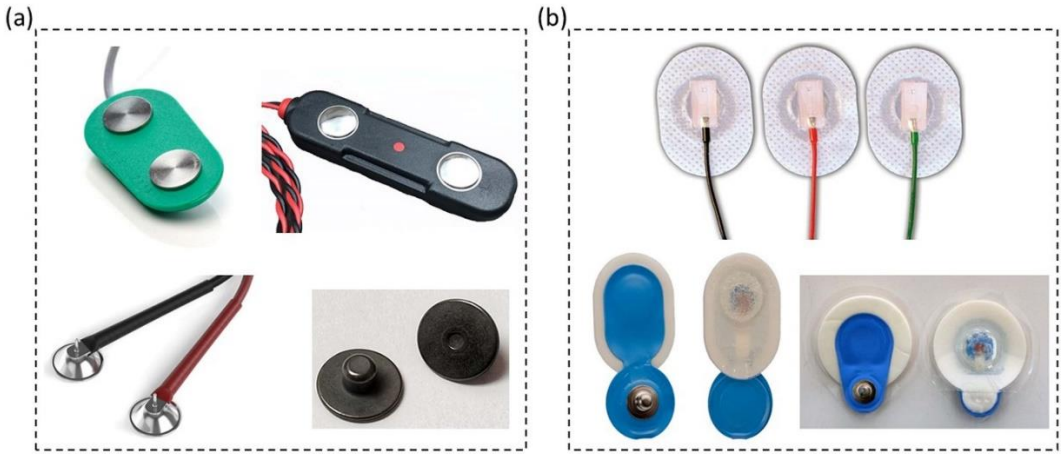

Figure 3.1 (a) Dry type surface myoelectrodes, (b) wet type surface myoelectrodes.

Pascal laferriere et al, 2011 proposed dry flexible electrodes and compared their performance with the commercial Ag/AgCl electrodes for detecting muscle contractions under different loading conditions (Laferriere, Lemaire, and Chan 2011). A finely machined toothed silver electrode was developed for acquiring EMG signal, which showed performances similar to gelled type electrode and better than the flat silver surface (Jamal and Kim 2018).

Myoelectric prosthesis requires a sensor that can reliably capture surface Electromyography (sEMG) signals from amputees for its controlled operation. The main problems with the presently available EMG devices are their extremely high cost, large response time, noise susceptibility, less amplitude sensitivity, larger size, and inability to provide the open-source platform (Supuk, Skelin, and Cic 2014; Imtiaz et al. 2013; Drost et al. 2006; Farina et al. 2014; Farrell and Weir 2007; Milosevic, Benatti, and Farella 2017). Moreover, the performance of the majority of available EMG devices is based on wet type electrodes, which cannot be used for long-term prosthetic applications. Some commercially available EMG sensors based on dry and wet type electrodes are already described in Table 2.1 of chapter 2.

This chapter describes the development of a dry electrode-based compact sEMG sensor for the application of hand prostheses. The sensor consists of an electrode interface, signal conditioning unit, and power supply unit, all encased in a single package. The sensor is an upgraded version of the earlier developed sensor (described in chapter 2). The performance of dry electrodes employed in the electrode interface was analyzed with the conventional Ag/AgCl electrodes. Moreover, the output performance of the developed sensor was compared with commercial EMG sensor regarding the signal-to-noise ratio (SNR), sensitivity, and response time. Finally, the developed sEMG sensor was further tested on amputees to control the operation of a self-designed 3D printed prosthetic hand.

3.2 Materials and Methods

3.2.1 Design and development of sEMG sensor

The proposed sEMG sensor mainly consists of silver palette electrodes as an electrode interface, a signal conditioning section, and a power supply unit embedded in a single structure. Figure 3.2(a) shows the block diagram of the proposed sEMG sensor. Except for the electrode interface, the other units like the conditioning circuitry and power supply of this sensor were similar to that of the earlier developed sensor (described in chapter 2).

3.2.1.1 Fabrication of electrode interface

The skin interface of the sensor was designed using three silver palette electrodes of 1.24 cm diameter each. The electrodes were embedded in the sensor base at an inter-electrode distance of 1.25 cm, shown in Figure 3.3(b). The two electrodes at the end position are intended for target muscles, while the middle electrode serves as a reference to make the whole arrangement a differential one. This electrode configuration minimizes the motion artifacts due to electrode cables' movement (Gerdle et al. 1999). Silver metal as a surface myoelectrode serves several advantages such as the good property of biosignal conduction and biocompatibility, does not require skin preparation, works well under sweat and wet conditions, cheaper for long-term use, non-toxic and non-reactive. (Searle and Kirkup 2000; Laferriere, Lemaire, and Chan 2011; Jamal and Kim 2018).

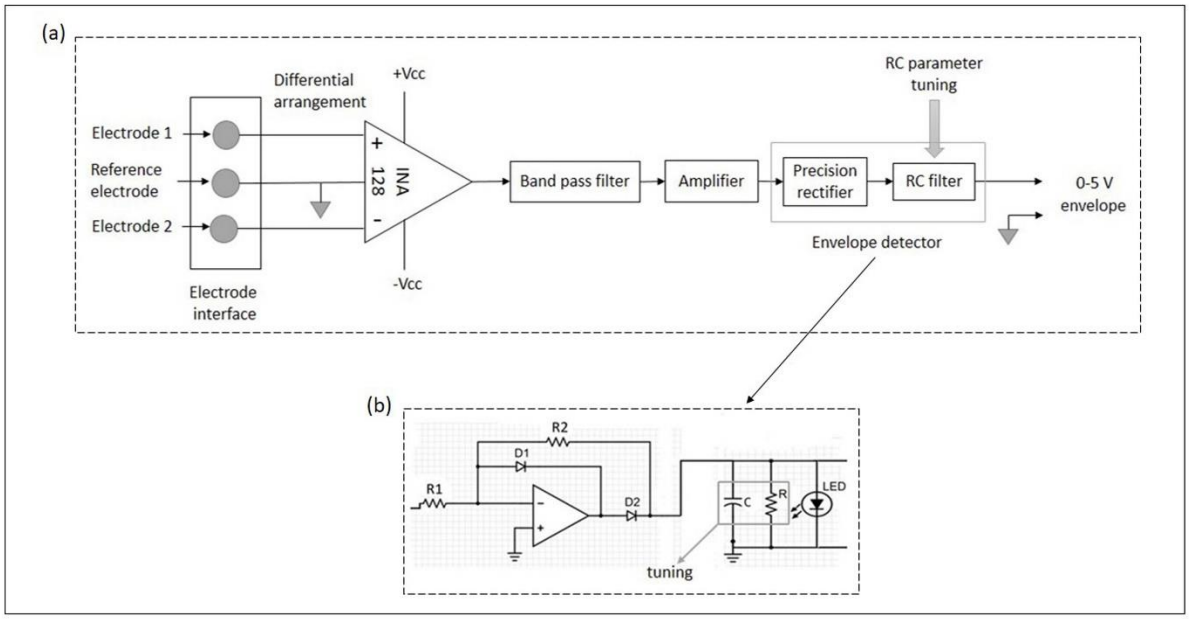

Figure 3.2 (a) Block diagram representation of the proposed EMG sensor, (b) detailed circuit for the envelope detector.

3.2.1.2 Design of preprocessing circuitry

A signal conditioning circuitry consisting of a preamplifier, a band-pass filter, inverting amplifier, and envelope detector was designed to convert the raw sEMG signal directly from the electrodes to an even voltage signal (similar to chapter 2). Figure 3.2(a) and 3.2(b) describe the different stages of the EMG signal conditioning unit.

3.2.1.3 Sensor description

Figure 3.3(a) describes the front view of the sensor comprising the signal conditioning circuitry and power supply unit, whereas Figure 3.3(b) depicts the rear view of the sensor, i.e., sensor base showing the electrode interface. The dimension of the developed sensor is 25×70 mm^2, which can be further reduced (up to one-third of the original dimension) by using small size SMD (surface-mount devices) components and professional tools for fabrication. The power consumption of the developed sensor was estimated 30 mA using the datasheets of the components employed in the circuitry.

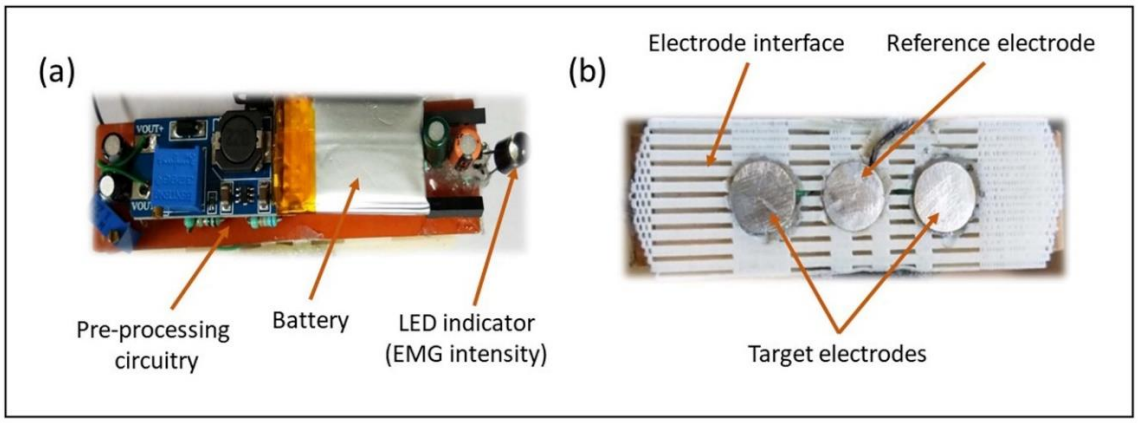

Figure 3.3 (a) Front view of the developed sensor, (b) Rear view of the developed sensor.

3.2.2 Experimental setup for Assessment of sensor performance

3.2.2.1 Selection of sensor for comparison

The performance of the developed sEMG sensor was validated by comparing its output parameters with the conventional EMG sensor. Specifications mentioned in Table 2.1 (chapter 2) show that Ottobock 13E200 and myoware muscle sensor are the two devices that provide similar output as the developed sensor. Myoware muscle sensor was preferred for comparison due to its low cost, availability and application in prosthetics (Tavakoli, Benussi, and Lourenco 2017).

S.no.	Gender	Age	Weight	Type of Amputation	Reason of Amputation
1.	Male	20	50 kg	Transradial(left hand)	Accident
2.	Male	50	85 kg	Transradial(right hand)	Accident
3.	Male	12	25 kg	Transradial(right hand)	Accident

Table 3.1 Details of amputees participated in EMG data acquisition.

EMG data were acquired from a total of ten subjects (three amputees and seven intact) using both sensors for determining their output parameters. Ethical approval was taken from the

Ethical Committee, Institute of medical sciences, BHU, Varanasi before performing this experiment. Details of each amputee who participated in this work with their type and the reason for amputation are described in Table 3.1.

3.2.2.2 Positioning of sensors

For acquiring the EMG data, both the sensors were attached to the forearm muscles of subjects, as shown in Figure 3.4. The developed sensor is dry electrode-based; it was attached using velcro tape, whereas the myoware muscle sensor was fixed through disposable Ag/AgCl electrodes. The target electrodes of both the sensors were placed at flexor carpi radialis and flexor carpi ulnaris, while the reference electrode of the myoware sensor was placed at the elbow portion. These specified muscle groups on the forearm are directly responsible for the palm and wrist movements of interest (Supuk, Skelin, and Cic 2014).

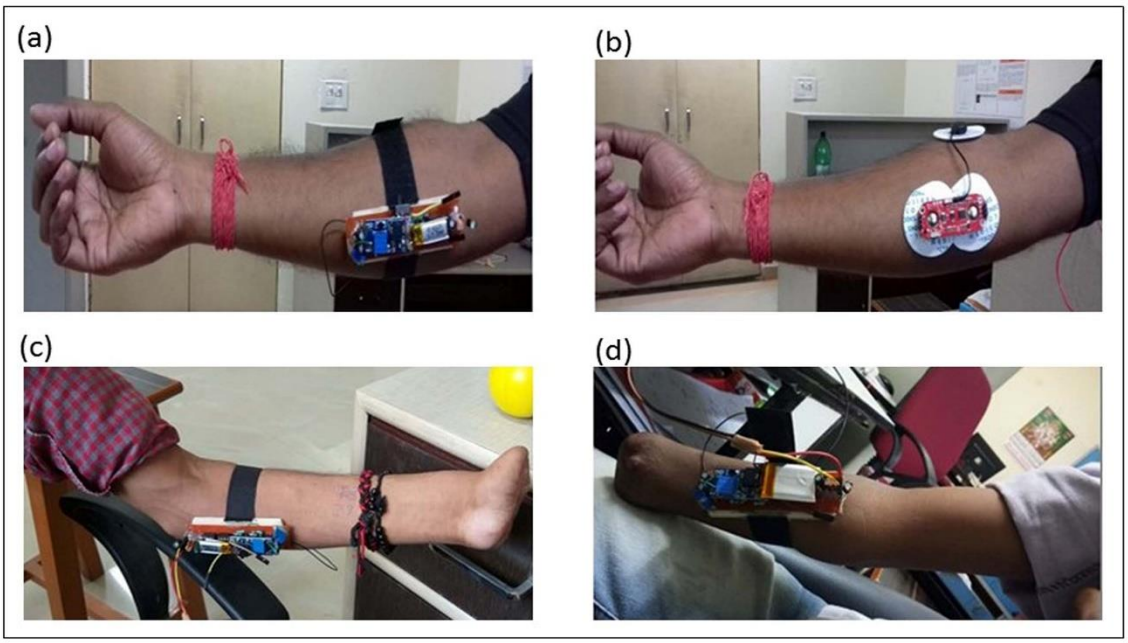

Figure 3.4 Attachment of (a) developed sensor on the healthy subject, (b) conventional sensor on the healthy subject, (c), (d) developed sensor on amputees.

3.2.2.3 Defining the level of muscular contraction

The EMG data for all the subjects were recorded for a different level of contractions (i.e., contractile force) of their forearm muscles. As the amputees cannot perform natural hand activities with their residual limb, the same activities were decided for amputees and healthy subjects to maintain uniformity in EMG data. The different levels of contractile force were selected from the force exerted by flexor muscles on the force-sensitive resistor (FSR) during contraction. A highly sensitive band comprising FSR was developed to measure muscular contractile force in terms of voltage. The FSR sensing portion was encased in a 3D printed structure to properly distribute muscular contractile force over the contact surface area. Figure 3.5 shows the sensing area of the designed FSR band, its voltage divider circuit for converting the change in resistance of FSR to voltage output and its attachment to the forearm for measuring contractile force. Using the force curve from the FSR datasheet (FSR 406) and circuit in Figure 3.5(b), a force voltage calibration curve was obtained, which is shown in Figure 3.6 ("FSR Integration Guide - Interlink Electronics | DigiKey"). A maximum of six different muscular contractions were defined for recording EMG data from the obtained calibration curve, as indicated in Table 3.2. The output voltage of the 6^{th} level corresponds to the maximum voluntary contraction (MVC) of the forearm muscle. Attachment of developed sensor and FSR band was done together on the forearm muscles as shown in Figure 3.5(d) for recording EMG signal at different contraction levels.

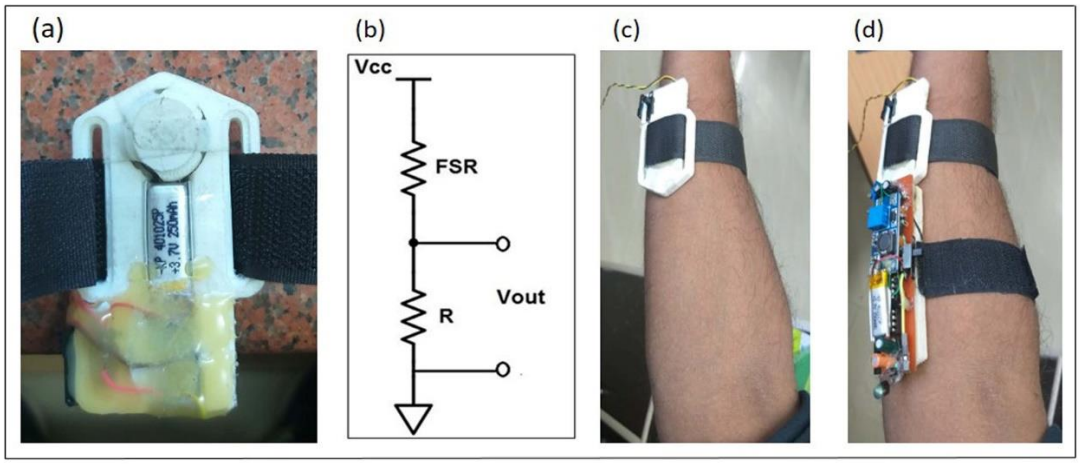

Figure 3.5 (a) Sensing area of the FSR band, (b) Output circuit for the band, (c) Attachment of band to the forearm, (d) Attachment of the developed sensor and band together to the forearm.

FSR output voltage (V)	Force (N)	Contraction level
0.8	0.18	1
1.25	0.2	2
1.7	0.3	3
2.2	0.5	4
2.8	1	5
3.2	2.5	6

Table 3.2 Contraction level determined from FSR output.

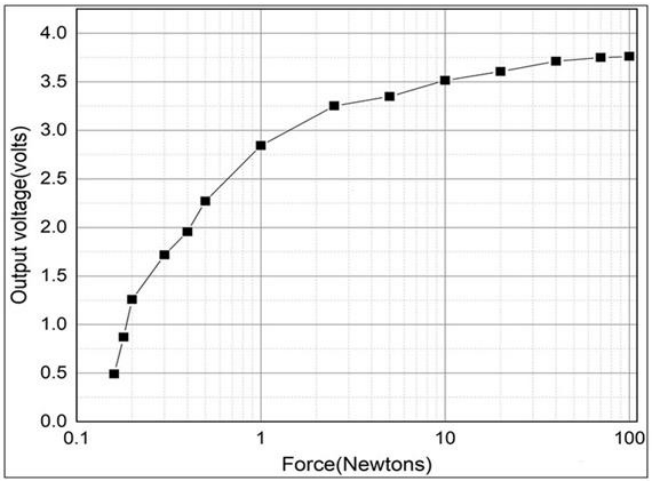

Figure 3.6 Force voltage calibration curve for FSR band.

3.2.2.4 Data acquisition

EMG data acquisition was performed using NI ELVIS II^+ hardware and Lab VIEW 2015 software interface. As per the levels defined in Table 3.2, the subjects were asked to perform six different levels of muscular contractions of their forearm, and ten repeated readings were recorded for each level. The duration of each reading was 6 seconds. All the data were acquired at a sampling rate of 2 kS/s.

3.3 Results and discussion

The developed EMG sensor mainly depends on the performance of the electrode interface and the employed signal conditioning circuitry. Therefore, there are several measures used to quantify the quality of electrodes. The most prominent are electrode-skin contact impedance and signal-to-noise ratio (SNR) (Konrad, 2005).

Similarly, the overall output performance of the developed sensor can be analyzed by various characteristics like SNR, amplitude sensitivity, and response time. Therefore the performance parameters of the proposed electrode and the sensor were separately determined and compared with that of the standard system.

3.3.1 Electrode performance

The performance of silver palette electrodes embedded in the sensor was compared with the standard disposable Ag/AgCl electrodes regarding electrode-skin impedance and signal-to-noise ratio (SNR).

3.3.1.1 Electrode-skin impedance

Grimnes's method was used for determining the electrode-skin impedance of individual surface electrodes (Grimnes 1983). A constant sinusoidal current of 50 µA at 50 Hz (generated

by a voltage-controlled current source) was passed through the skin from one electrode and exited from the other. The impedance values for the proposed electrodes and disposable electrodes were obtained and recorded using Lab VIEW with NI ELVIS II^+ hardware interface at a sampling frequency of 2 kS/s. The location of both the electrodes was kept the same for the measurement of each impedance. Impedance vs. time plot for both the electrodes was obtained using the recorded data for 15 minutes. The impedance values for the proposed electrode showed a decrease over time, which is quite clear from Figure 3.7. In general, a lower impedance is desired for better conduction of electrodes (Konrad, 2005). A comparison regarding observed impedance values for both electrodes is provided in Table 3.3. After a certain settling time, dry metal electrodes show comparable impedance values to wet type electrodes (Searle and Kirkup 2000).

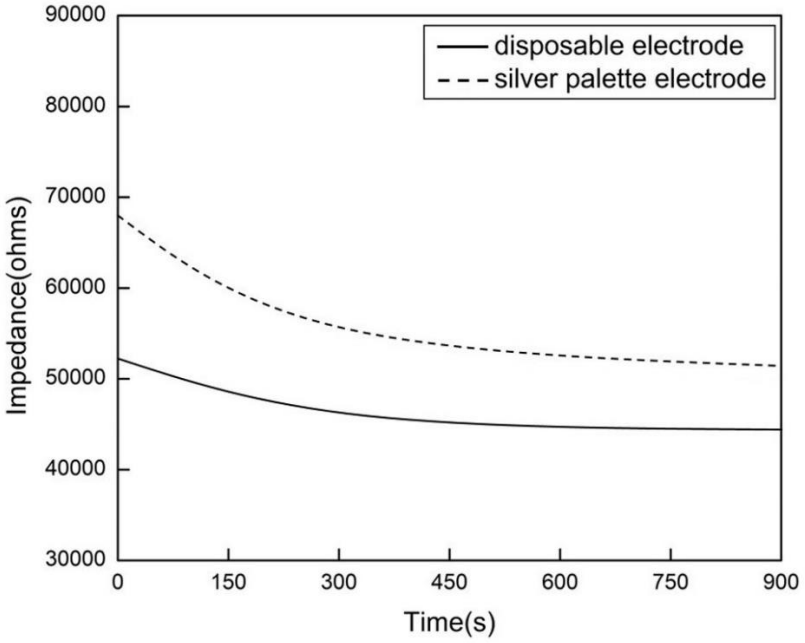

Figure 3.7 Obtained impedance response for both the surface electrodes.

3.3.1.2 Electrode SNR

Assessment of noise performance of the proposed electrode was analyzed through evaluation of signal-to-noise ratio (SNR). SNR was determined as the ratio of root mean square (RMS) value of raw EMG signal recorded during muscular contraction to the RMS value of the undesired signal (i.e., baseline noise) recorded while the muscle is at rest (Agostini and Knaflitz 2012). The raw EMG signals with both the electrodes were recorded for maximum voluntary contraction (MVC) of the forearm muscle, whereas the undesired signals were recorded for no contraction. The data of 6 s duration were acquired for each subject. The SNR value was evaluated for each subject using equation (3.1). Average SNR values of all the subjects determined for both the electrodes are mentioned in Table 3.3. The table shows that the proposed electrode provides similar SNR values as the conventional Ag/AgCl electrode.

$$SNR = 20\ log_{10}\left(\frac{RMS_{signal}}{RMS_{noise}}\right) \tag{3.1}$$

S.No.	Type of electrode	Area (mm^2)	Impedance (kΩ)	SNR (dB)
1	Disposable Ag/AgCl	314	48	24.4
2	Silver palette	120	59	26.7

Table 3.3 Performance comparison for surface electrodes.

3.3.2 Sensor overall performance

3.3.2.1 Output

Figure 3.8 shows the EMG signals for six different levels of muscular contractions (i.e., activities) of an amputee recorded with both the sensors. To quantitatively analyze the similarity between the signals of both the sensors, a two-tailed paired t-test was conducted. The similarity test was performed using EMG data of all the ten subjects considering their

every level of muscular contraction separately. The result showed a high Pearson's correlation coefficient ($r > 0.95$) with a p-value < 0.0001, revealing the pairing was significantly effective.

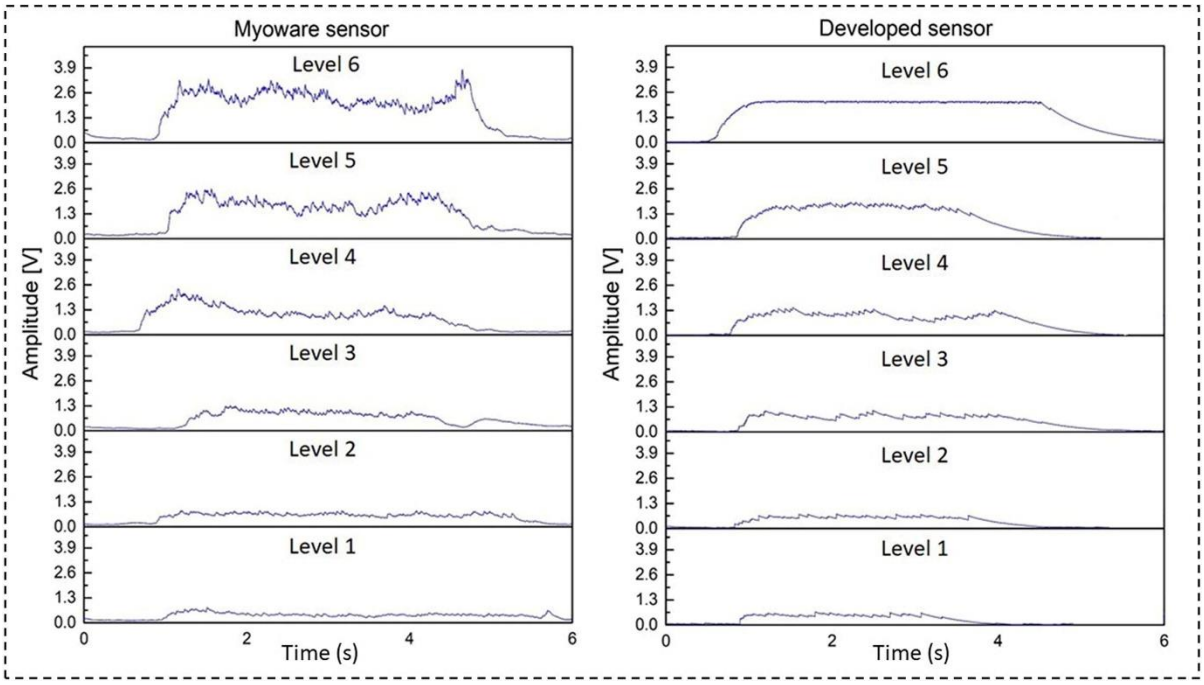

Figure 3.8 Envelopes produced by the two sensors for six different levels of muscular contractions of an amputee.

3.3.2.2 SNR

To analyze the signal quality of both the sensors, their SNR values were determined. EMG signals using both the sensors were acquired for the same contractile force of the forearm muscle (i.e., for MVC), while noises were acquired for no contraction. Figure 3.9(a) shows an EMG waveform indicating baseline noise and signal strength, whereas Figure 3.9(b) and 3.9(c) describe the recorded baseline noises for a subject with both sensors. For each subject, the SNR value was calculated using equation (2), considering data of 6 s duration. Table 3.4 gives the evaluated SNR values for all the subjects with both sensors. In the results, higher SNR values were observed for the developed sensor than the commercial sensor. SNR measures the quality of the EMG signal and can range between 10 dB to 50 dB under ideal, simulated situations (Sinderby, Lindström, and Grassino 1995).

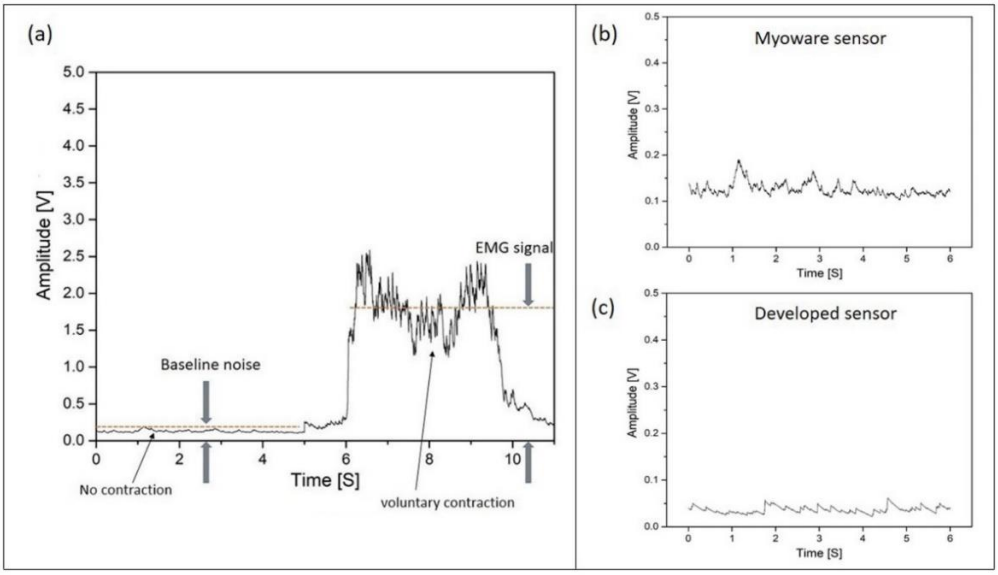

Figure 3.9 (a) SNR calculation from recorded EMG envelope, (b) Baseline noise for myoware sensor, (c) Baseline noise for the developed sensor.

Subject	Sensor	SNR(dB)
1	developed	31.86
	myoware	24.08
2	developed	30.46
	myoware	23.32
3	developed	30.66
	myoware	22.92
4	developed	31.23
	myoware	23.52
5	developed	32.02
	myoware	22.49
6	developed	32.20
	myoware	23.20
7	developed	32.32
	myoware	23.86

8	developed	31.25
	myoware	23.36
9	developed	32.17
	myoware	23.93
10	developed	30.47
	myoware	23.24
Average value	developed	31.46
	myoware	23.39

Table 3.4 Evaluated SNR by sensor type.

3.3.2.3 Sensitivity

Sensitivity analysis was performed for both the sensors to test the ability of the developed sensor module in detecting EMG amplitude variations from various subjects. Amplitude sensitivity for the sensors was evaluated as the ratio of incremental change in the EMG output voltage to the change in the muscular contractile force (i.e., input to the EMG sensor) (Thuau et al. 2014; Rodrigues et al. 2017). A plot was obtained for a corresponding change of average EMG voltage (for subjects) with a change in muscle contractile force for both the sensors. The slope of the obtained linear curve was calculated to give the sensitivity of the sensor. Fig. 3.10(a) and 3.10(b) show the sensitivities of both the sensors for all the subjects and only amputees. The results showed that the developed sensor was 45% more sensitive than the myoware sensor in detecting the signal from all the subjects, whereas in the case of only amputees, it was 70% more sensitive than the myoware muscle sensor. Sensitivities of both the sensors were determined at a fixed gain value at which their SNR is maximum. Because as

we increase the gain of an EMG system above a certain value, its baseline noise increases, which decreases the SNR value of the system (Agostini and Knaflitz 2012).

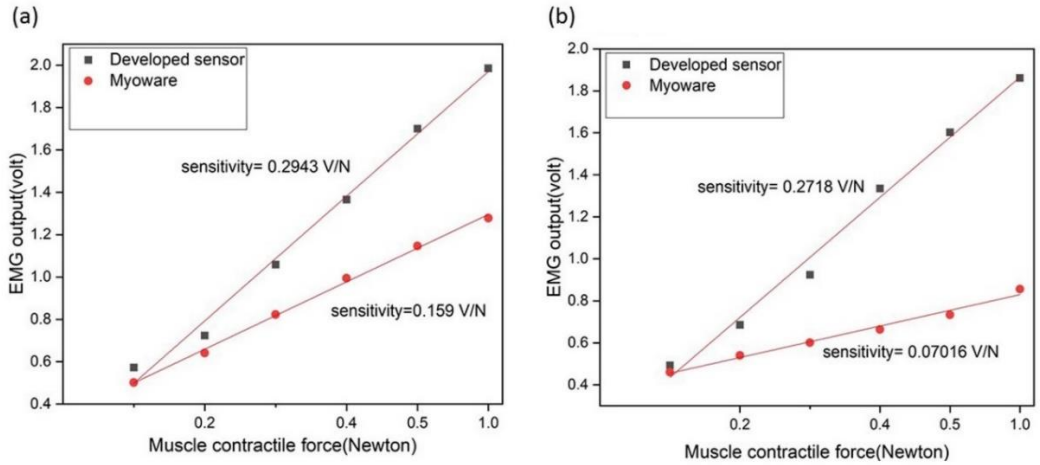

Figure 3.10 (a) Sensitivities of sensors for all the subjects, (b) Sensitivities of sensors for only amputees.

3.3.2.4 Response time

The sensor's response time was evaluated in terms of its output envelope's rise and fall time. Rise time was measured as the time required for the envelope to rise from 10% to 90% of its largest value. Conversely, fall time was calculated as the time taken by the envelope to fall from 90% to 10% of its maximum value (Greene and Lo 1998). Figure 3.11 shows the estimation of rise and fall time from the produced EMG envelope. Rise and fall time was computed from the EMG envelopes generated with both the sensors placed at the same muscle group for similar contractile force. For each subject, response times were determined for all the six levels of muscular contractions (defined in Table 3.3) using both sensors.

In Table 3.6, the first six rows indicate the average rise and fall time calculated for each contraction level considering all the subjects, while the last row gives the overall rise and fall time for the sensors. The rise time for the developed sensor was obtained to be 57% faster (lower) than the myoware sensor, whereas the fall time for the sensor was observed 36% higher

in comparison to the commercial sensor. The charging and discharging time constant of the RC filter circuit mainly regulates the rise and fall time and the shape of the generated envelope (Balbinot and Favieiro 2013). Therefore, the value of R and C in the envelope detector stage was adjusted manually to obtain a smooth and faster EMG signal with lower rise time and higher fall time. Since the myoelectric control signal has a delay time of about 300 ms from the time when user intention is given, the rise time of the developed sensor is suitable for the intuitive application (Hudgins, Parker, and Scott 1993; Farrell and Weir 2007; Englehart, Hudgin, and Parker 2001).

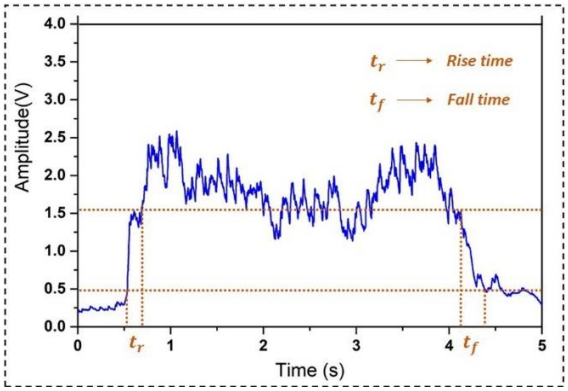

Figure 3.11 Rise and fall time calculation from an EMG envelope.

Muscular contraction level	Rise time, t_r (ms)		Fall time, t_f (ms)	
	Myoware	Developed sensor	Myoware	Developed sensor
1	260	110	190	300
2	280	110	220	360
3	310	130	230	390
4	340	140	270	430
5	370	160	310	480
6	380	170	350	490
Average	323	136	261	408

Table 3.5 Rise and fall time for both the sensors.

3.4 Sensor utilization for prosthetic hand control

The developed sensor was further utilized to control the operation of a 3D printed prosthetic hand by capturing the EMG signal from amputees. A 3D printed hand prototype was prepared and intrinsically actuated using two high torque servomotors (MG-995) (Kargov et al. 2004). Fingers were equipped with silicon fingertips for improving the grasping capability of the hand. A microcontroller chip (Arduino Nano) was installed inside the hand, which receives analog input from the EMG sensor and provides a digital output to servomotors. All the electrical and electronic components present within the hand were powered using a 2000 mAh lithium-ion battery.

The proportional control strategy was implemented in the microcontroller section, which translates the EMG signal from the sensor to PWM output for driving servomotor. This strategy provides proportional actuation of the prosthetic hand fingers as per the intensity of the EMG signal, i.e., larger strength of EMG signal corresponds to the greater grasping force of fingers to close the hand. Figure 3.12 shows the scheme for the generation of control commands for real-time operation of the 3D printed prosthetic hand.

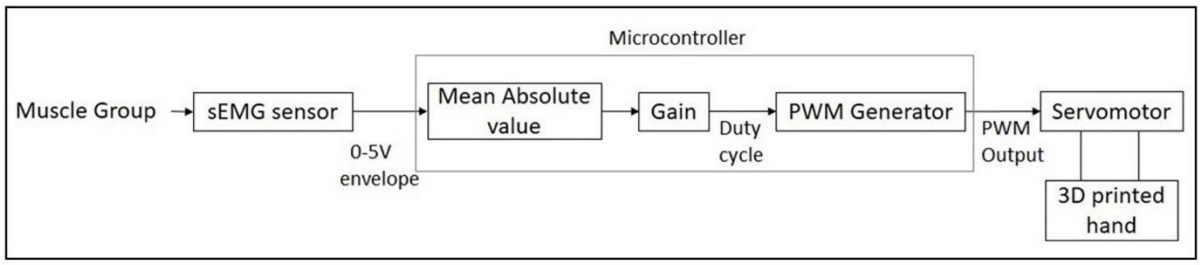

Figure 3.12 Generation of control command using EMG signal from the sensor.

The sEMG sensor was attached to the residual forearm stump of amputees, as shown in Figure 3.4, for real-time control of the designed prosthetic hand. The amputees were able to dexterously grasp different shaped objects with the hand using their muscular contractions (i.e.,

the intensity of EMG signal). Figure 3.13 shows the grasping of various objects with the prosthetic hand, using EMG signals from an amputee.

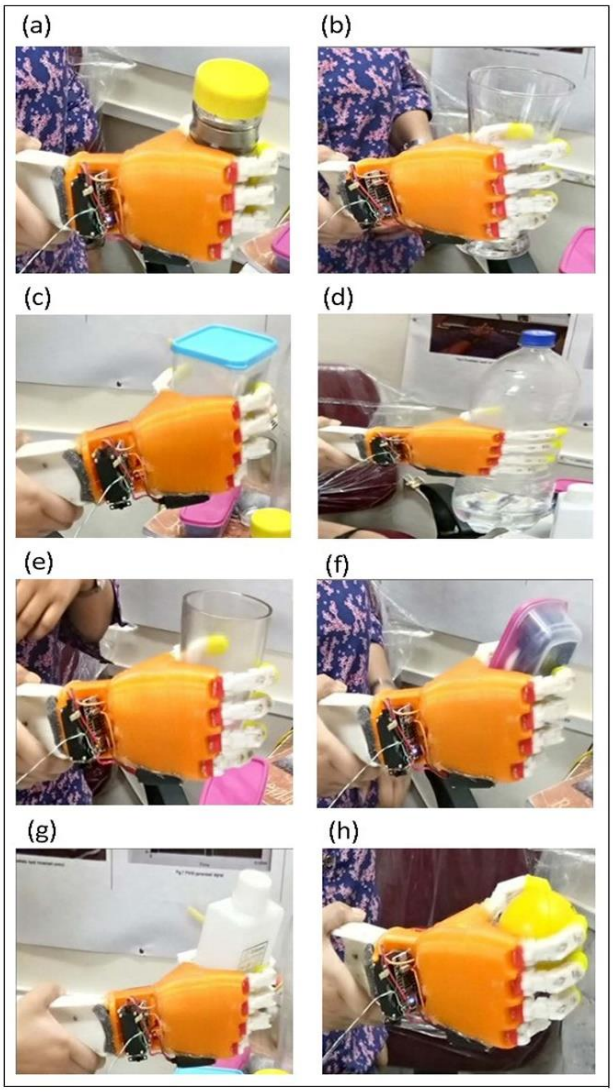

Figure 3.13 Grasping of various objects performed by prosthetic hand using EMG signals from an amputee.

The proportional myoelectric control provides the operating speed of the prosthetic hand that is dependent on the intensity of the EMG signal. This feature enables intuitive control and faster-grasping capability to the hand (Lenzi et al. 2012; Fougner et al. 2012; Geethanjali 2016). The operation speed of the myoelectric hand setup was analyzed in terms of its response time. In addition, an experiment was performed in which response time (i.e., Closing/opening

time) of the prosthetic hand with both the sensors was determined from their recorded video of hand operation. The full closing and full opening time of prosthetic hand fingers with both the sensors are provided in Table 3.7. Faster closing and slower opening operation of the prosthetic hand was observed with the developed sensor compared to the myoware sensor. Based on the survey report of amputees, researchers recommended 300-400 ms as the acceptable closing time for the myoelectric prosthesis (Farrell and Weir 2007; Englehart, Hudgin, and Parker 2001; Belter et al. 2013).

Prosthetic hand	**Full closing time (ms)**	**Full opening time (ms)**
With developed sensor	350	650
With myoware muscle sensor	550	450

Table 3.6 Response time of hand with both the sensors.

The operating speed of the prosthetic hand is primarily regulated by the combined effect of EMG sensor delay, microcontroller processing time, and the response time of the servomotor. The processing time of the Arduino nano microcontroller (in generating control command) and response time of the servomotor (MG-995) as per their datasheets are 40 ms and 160 ms (Farrell and Weir 2007). Therefore, analyzing Tables 3.6 and 3.7, the closing time of the hand mainly depends on the rise time of the EMG sensor envelope. Conversely, the opening time depends on the fall time of the envelope.

3.5 Conclusion

In this chapter, a dry electrode-based sEMG sensor has been designed for upper limb prosthetic application. The compact structure of the sensor makes it wearable for a long time used inside the prosthetic hand socket. Furthermore, the Silver palette electrodes used in the sensor showed

decent performance, i.e., electrode-skin impedance and SNR values compared to the standard Ag/AgCl electrodes. The developed sensor showed better output parameters such as SNR, sensitivity, and response time than the commercial sensor. A comparison of full features between a commercial sensor, a developed sensor with Ag/AgCl electrodes (in chapter 2) and a developed sensor with dry electrodes are presented in Table 3.8.

Features	**Myoware muscle sensor**	**Developed EMG sensor**	**Developed EMG sensor with dry electrodes**
Output type	0-5 V EMG envelope	0-5 V EMG envelope	0-5 V EMG envelope
Electrode type	Disposable Ag/AgCl	Disposable Ag/AgCl	Silver palette
Inter-electrode distance	2.5 cm	4 cm	1.25 cm
Power supply unit	external	integrated	integrated
Power consumption	9 mA	25 mA	30 mA
Mass	9 g	45 g	42 g
Dimension	20×52 mm^2	35×70 mm2	25×70 mm^2
SNR	23.39 dB	32.68 dB	31.46 dB
Sensitivity	0.159 V/N	0.3944 V/N	0.2943 V/N
Rise time	323 ms	136 ms	136 ms
Fall time	261 ms	440 ms	408 ms
Price in the commercial market	$37.95	Prototyping cost($13)	Prototyping cost($15)

Table 3.7 Specification for the sensors.

The sensor was successfully tested on amputees for the real-time controlled operation of the developed prosthetic hand. Implementation of a proportional control scheme enables the grasping force of the hand fingers proportional to the EMG signal strength. Based on their EMG signal intensity, amputees were able to grasp different shaped objects with the hand.

The higher sensitivity with greater SNR values of the developed sensor facilitates reliable detection of sEMG signal from subjects (particularly amputees) and yields smoother operation of the prosthetic device. The operating speed (i.e., closing/opening time) of the prosthetic hand is highly influenced by the sensor's response time (i.e., rise and fall time). The lower (faster) rise time of the sensor offers faster closing of the prosthetic hand fingers to grasp the objects (when the muscle is activated), whereas higher fall time provides some delay in the opening of hand fingers to prevent the immediate release of grasped objects (when the muscle is instantly relaxed). The tuning of RC parameters in the envelope detection stage of the sensor was mainly responsible for the generation of a smoother envelope with lower rise time and higher fall time. Thus, the developed EMG sensor implemented with proportional control strategy provided smooth and faster operation of a prosthetic hand with control on grasp force.

The dry electrodes integrated into the skin interface of the sensor offers several benefits over the conventional Ag/AgCl electrodes, such as cheap for longer-time use, does not require any skin preparation, does not cause allergies and skin irritation when used for a longer duration, signal quality remains consistent over time, good performance under sweat and wet conditions etc. Also, a power supply within the sensor eradicates the need for an external bipolar supply, creating complexity to the acquisition setup. The power consumption of the developed sensor is higher than the myoware sensor; however, with a rechargeable battery of 350 mAh, it can last up to 11 hours of continuous use. Larger mass and dimension are some demerits of the designed sensor, which can be overcome by using tiny-sized SMD components and specialized tools for fabrication.

In future work, the EMG signals acquired with the sensor for different muscular contraction levels can be easily classified to achieve individual finger movement of the prosthetic hand.

This approach will enhance the number of grip patterns for a more precise and natural grasping of objects. Also, such a simple, effective, and low-cost sensor can be utilized to develop the affordable myoelectric hand.

3.6 References

Agostini, V., and M. Knaflitz. 2012. "An Algorithm for the Estimation of the Signal-To-Noise Ratio in Surface Myoelectric Signals Generated During Cyclic Movements." *IEEE Transactions on Biomedical Engineering* 59 (1): 219–25. https://doi.org/10.1109/TBME.2011.2170687.

Baek, Ju-Yeoul, Jin-Hee An, Jong-Min Choi, Kwang-Suk Park, and Sang-Hoon Lee. 2008. "Flexible Polymeric Dry Electrodes for the Long-Term Monitoring of ECG." *Sensors and Actuators A: Physical* 143 (2): 423–29. https://doi.org/10.1016/j.sna.2007.11.019.

Balbinot, Alexandre, and Gabriela Favieiro. 2013. "A Neuro-Fuzzy System for Characterization of Arm Movements." *Sensors (Basel, Switzerland)* 13 (2): 2613–30. https://doi.org/10.3390/s130202613.

Belter, Joseph T., Jacob L. Segil, Aaron M. Dollar, and Richard F. Weir. 2013. "Mechanical Design and Performance Specifications of Anthropomorphic Prosthetic Hands: A Review." *The Journal of Rehabilitation Research and Development* 50 (5): 599. https://doi.org/10.1682/JRRD.2011.10.0188.

Drost, Gea, Dick F. Stegeman, Baziel G. M. van Engelen, and Machiel J. Zwarts. 2006. "Clinical Applications of High-Density Surface EMG: A Systematic Review." *Journal of Electromyography and Kinesiology: Official Journal of the International Society of Electrophysiological Kinesiology* 16 (6): 586–602. https://doi.org/10.1016/j.jelekin.2006.09.005.

Englehart, K., B. Hudgin, and P. A. Parker. 2001. "A Wavelet-Based Continuous Classification Scheme for Multifunction Myoelectric Control." *IEEE Transactions on Biomedical Engineering* 48 (3): 302–11. https://doi.org/10.1109/10.914793.

Farina, Dario, Ning Jiang, Hubertus Rehbaum, Aleš Holobar, Bernhard Graimann, Hans Dietl, and Oskar C. Aszmann. 2014. "The Extraction of Neural Information from the Surface EMG for the Control of Upper-Limb Prostheses: Emerging Avenues and Challenges." *IEEE Transactions on Neural Systems and Rehabilitation Engineering: A Publication of the IEEE Engineering in Medicine and Biology Society* 22 (4): 797–809. https://doi.org/10.1109/TNSRE.2014.2305111.

Farrell, Todd R., and Richard F. Weir. 2007. "The Optimal Controller Delay for Myoelectric Prostheses." *IEEE Transactions on Neural Systems and Rehabilitation Engineering: A Publication of the IEEE Engineering in Medicine and Biology Society* 15 (1): 111–18. https://doi.org/10.1109/TNSRE.2007.891391.

Fougner, Anders, Oyvind Stavdahl, Peter J. Kyberd, Yves G. Losier, and Philip A. Parker. 2012. "Control of Upper Limb Prostheses: Terminology and Proportional Myoelectric Control-a Review." *IEEE Transactions on Neural Systems and Rehabilitation Engineering: A Publication of the IEEE Engineering in Medicine and Biology Society* 20 (5): 663–77. https://doi.org/10.1109/TNSRE.2012.2196711.

"FSR Integration Guide - Interlink Electronics | DigiKey." n.d. Accessed June 15, 2019. https://www.digikey.com/en/pdf/i/interlink-electronics/interlink-electronics-fsr-force-sensing-resistors-integration-guide.

Geethanjali, Purushothaman. 2016. "Myoelectric Control of Prosthetic Hands: State-of-the-Art Review." *Medical Devices (Auckland, N.Z.)* 9: 247–55. https://doi.org/10.2147/MDER.S91102.

Gerdle, Björn, Stefan Karlsson, Scott Day, and Mats Djupsjöbacka. 1999. “Acquisition, Processing and Analysis of the Surface Electromyogram.” In *Modern Techniques in Neuroscience Research*, edited by Uwe Windhorst and Håkan Johansson, 705–55. Berlin, Heidelberg: Springer Berlin Heidelberg. https://doi.org/10.1007/978-3-642-58552-4_26.

Greene, Elliott J, and Pei-Hwa Lo. 1998. “RISE TIME, FALL TIME AND PULSE WIDTH,” 6.

Grimnes, S. 1983. “Impedance Measurement of Individual Skin Surface Electrodes.” *Medical & Biological Engineering & Computing* 21 (6): 750–55. https://doi.org/10.1007/BF02464038.

Hudgins, B., P. Parker, and R.N. Scott. 1993. “A New Strategy for Multifunction Myoelectric Control.” *IEEE Transactions on Biomedical Engineering* 40 (1): 82–94. https://doi.org/10.1109/10.204774.

Imtiaz, U., L. Bartolomeo, Z. Lin, S. Sessa, H. Ishii, K. Saito, M. Zecca, and A. Takanishi. 2013. “Design of a Wireless Miniature Low Cost EMG Sensor Using Gold Plated Dry Electrodes for Biomechanics Research.” In *2013 IEEE International Conference on Mechatronics and Automation*, 957–62. https://doi.org/10.1109/ICMA.2013.6618044.

Jamal, Muhammad Zahak, and Kyung-Soo Kim. 2018. “A Finely Machined Toothed Silver Electrode Surface for Improved Acquisition of EMG Signals.” In *2018 IEEE Sensors Applications Symposium (SAS)*, 1–5. Seoul: IEEE. https://doi.org/10.1109/SAS.2018.8336768.

Kargov, Artem, Christian Pylatiuk, Jan Martin, Stefan Schulz, and Leonhard Döderlein. 2004. “A Comparison of the Grip Force Distribution in Natural Hands and in Prosthetic Hands.” *Disability and Rehabilitation* 26 (12): 705–11. https://doi.org/10.1080/09638280410001704278.

Konrad, Peter. 2005. “A Practical Introduction to Kinesiological Electromyography,” 61.

Laferriere, Pascal, Edward D. Lemaire, and Adrian D. C. Chan. 2011. “Surface Electromyographic Signals Using Dry Electrodes.” *IEEE Transactions on Instrumentation and Measurement* 60 (10): 3259–68. https://doi.org/10.1109/TIM.2011.2164279.

Lenzi, T., S. M. M. De Rossi, N. Vitiello, and M. C. Carrozza. 2012. “Intention-Based EMG Control for Powered Exoskeletons.” *IEEE Transactions on Biomedical Engineering* 59 (8): 2180–90. https://doi.org/10.1109/TBME.2012.2198821.

Milosevic, B., S. Benatti, and E. Farella. 2017. “Design Challenges for Wearable EMG Applications.” In *Design, Automation Test in Europe Conference Exhibition (DATE), 2017*, 1432–37. https://doi.org/10.23919/DATE.2017.7927217.

Pylatiuk, C., M. Muller-Riederer, A. Kargov, S. Schulz, O. Schill, M. Reischl, and G. Bretthauer. 2009. “Comparison of Surface EMG Monitoring Electrodes for Long-Term Use in Rehabilitation Device Control.” In *2009 IEEE International Conference on Rehabilitation Robotics*, 300–304. Kyoto, Japan: IEEE. https://doi.org/10.1109/ICORR.2009.5209576.

Rodrigues, Domingos M. C., Rafaela N. Lopes, Marcos A. R. Franco, Marcelo M. Werneck, and Regina C. S. B. Allil. 2017. “Sensitivity Analysis of Different Shapes of a Plastic Optical Fiber-Based Immunosensor for Escherichia Coli: Simulation and Experimental Results.” *Sensors* 17 (12): 2944. https://doi.org/10.3390/s17122944.

Searle, A., and L. Kirkup. 2000. “A Direct Comparison of Wet, Dry and Insulating Bioelectric Recording Electrodes.” *Physiological Measurement* 21 (2): 271. https://doi.org/10.1088/0967-3334/21/2/307.

Shobaki, Mohammed M, Noreha Abdul Malik, Sheroz Khan, Anis Nurashikin, Samnan Haider, Sofiane Larbani, Atika Arshad, and Rumana Tasnim. 2013. “High Quality Acquisition of Surface Electromyography – Conditioning Circuit Design.” *IOP Conference Series: Materials Science and Engineering* 53 (December): 012027. https://doi.org/10.1088/1757-899X/53/1/012027.

Sinderby, C., L. Lindström, and A. E. Grassino. 1995. “Automatic Assessment of Electromyogram Quality.” *Journal of Applied Physiology (Bethesda, Md.: 1985)* 79 (5): 1803–15. https://doi.org/10.1152/jappl.1995.79.5.1803.

Supuk, Tamara Grujic, Ana Kuzmanic Skelin, and Maja Cic. 2014. “Design, Development and Testing of a Low-Cost SEMG System and Its Use in Recording Muscle Activity in Human Gait.” *Sensors (Basel, Switzerland)* 14 (5): 8235–58. https://doi.org/10.3390/s140508235.

Tavakoli, Mahmoud, Carlo Benussi, and Joao Luis Lourenco. 2017. “Single Channel Surface EMG Control of Advanced Prosthetic Hands.” *Expert Syst. Appl.* 79 (C): 322–32. https://doi.org/10.1016/j.eswa.2017.03.012.

Thuau, D., M. Abbas, S. Chambon, P. Tardy, G. Wantz, P. Poulin, L. Hirsch, I. Dufour, and C. Ayela. 2014. “Sensitivity Enhancement of a Flexible MEMS Strain Sensor by a Field Effect Transistor in an All Organic Approach.” *Organic Electronics* 15 (11): 3096–3100. https://doi.org/10.1016/j.orgel.2014.08.063.